

Draft proposal for the LHCb muon detector using RPC

M. Adinolfi^a, A. Bizzeti^b, G. Carboni^a, E. Iacopini^b, R. Messi^a,
L. Pacciani^a, L. Paoluzi^a, G. Passaleva^b, E. Santovetti^a

^a *Università degli Studi di Roma “Tor Vergata” and INFN, Roma, Italy*

^b *Università di Firenze and INFN, Firenze, Italy*

February 5, 2000

Abstract

We propose to use RPCs to equip a substantial part of the muon detector stations M2–M5. RPCs made of phenolic plates of low resistivity ($\rho = 9 \cdot 10^9 \Omega\text{cm}$) and operated in avalanche mode offer very good performance and several advantages in region IV of M2 and in regions III and IV of M3–M5. Using this technique it is possible to cover 90 % of the total area behind the calorimeters at moderate cost.

1 Introduction

The muon detector of experiment LHCb is made of 5 tracking stations, M1–M5. Resistive Plate Chambers (RPC) constitute a very attractive solution for equipping the outer region of stations M2–M5, located after the absorber, where the particle flux is relatively small [1]. RPCs are gaseous parallel-plate detectors that have several distinctive advantages, making them well suited for large-area fast trigger systems [2]. In summary we quote:

- robustness and simplicity of construction (no wires)
- excellent timing properties:
 - unambiguous bunch-crossing identification (resolution better than 2 ns)
 - negligible dead-time effects (in avalanche mode)
- well adapted to inexpensive industrial production.

The readout of RPCs occurs via capacitive coupling to external strip or pad electrodes, which are fully independent of the sensitive element (the gas gap). This constitutes a further advantage of the detector.

The weak point of RPCs was the rate capability, but recently progresses have been made along this direction. Shifting the operation mode to avalanche rather than streamer (see later) allowed to reach rate capabilities of several kHz/cm². In the LHCb muon detector the expected track density per cm² per interaction in stations M2 and M3 is shown in Fig. 1. In order to compute the particle flux, we multiply the curves by the interaction rate (10 MHz), and by a number of correction and safety coefficients yielding an overall factor 30¹ [3]. It is seen from

¹It has to be mentioned that these factors must be understood better. For example, the factor 2 (“dose/flux”) is probably redundant when using GIF data to evaluate the performances.

the plots that detectors in region IV of station M2 (starting at about 2 m from the beam) will need to stand a flux ≤ 2 kHz/cm². In stations M3–M5 the same limiting value is obtained around 1 m, corresponding to region III. RPC detectors built with low-resistivity phenolic plates can be used efficiently in these regions.

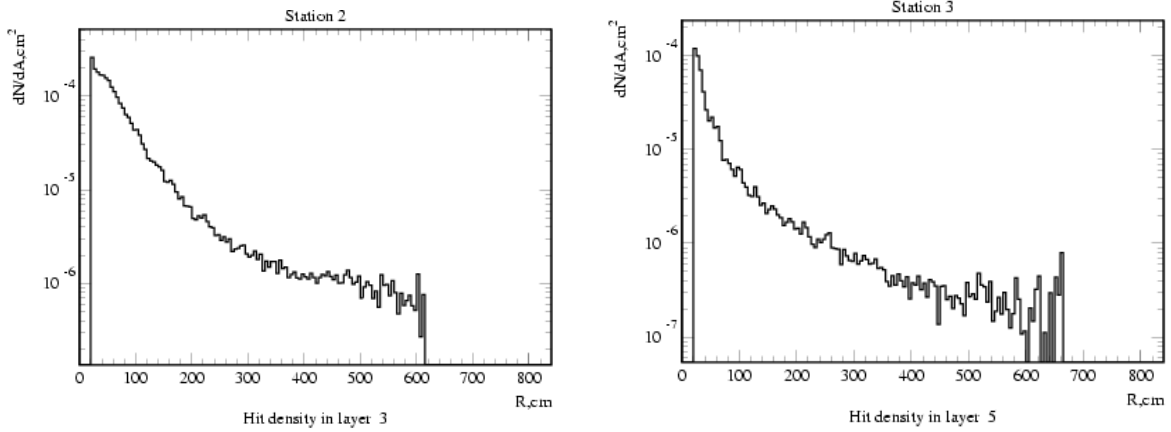


Figure 1 Charged track density/interaction in muon stations M2 and M3 (see text).

2 RPC detectors

2.1 Operating principles

2.1.1 Charge development

In Fig. 2 the working principle of the RPC is shown. Ionizing particles create electron-ion clusters in the gas, where an intense constant electric field is present between two parallel plates. An avalanche is created by multiplication in the gas, so that the cluster charge, q_0 , becomes $Q = q_0G(x) = q_0 \exp(\alpha x)$ after a distance x . α is the first Townsend coefficient and increases strongly with ratio of the electric field to the density. RPC operate at high gain, with $\langle G \rangle$ typically larger than 10^7 . This is necessary since, in order to have high efficiency, the multiplication factor must be large even for those clusters that are created close to the positive electrode. Dense gases with high Z are preferred since have larger ionization probability.

2.1.2 Signal characteristics

The moving and growing avalanche induces images currents on the readout electrodes. Given the characteristic exponential growth of the avalanche the output signal has a very fast risetime. Since the gain factor depends exponentially on x , a very large dynamic range results: typically the signal charge goes from 20 fC to 20 pC. A threshold of 20 fC is adequate to achieve full efficiency.

2.1.3 Streamer vs. avalanche mode

If the electric field is increased above a threshold which depends on the gas, the avalanche may be followed in time by a streamer. A rule of thumb says that this occurs when $\alpha d >$

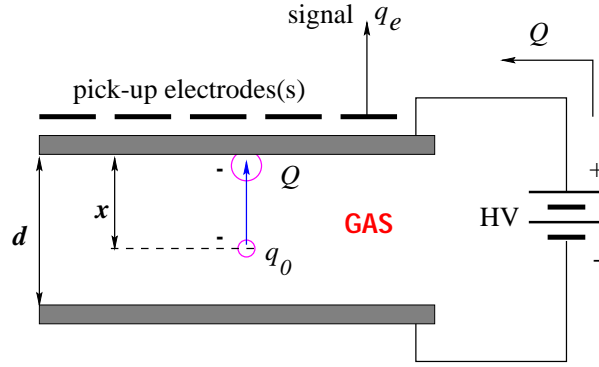


Figure 2 Principle of the RPC. Primary electron clusters, moving in the gas over a distance x , create an avalanche of final charge Q . A charge q_e is induced on the readout electrode(s).

20. The signal due to the streamers is much larger than the avalanche one, by at least one order of magnitude. In streamer mode the proportionality of the avalanche charge with the inducing charge is lost. When the electric field is further increased the avalanche-streamer delay decreases and the probability of generating streamers increases.

The presence of streamers was generally considered advantageous because the associated signal is large, however one must keep in mind that the avalanche (or the streamer) generated in the gas has the effect of discharging locally the electrodes. Thus a region around the trajectory of the ionizing particle becomes “blind” for a certain time until it is recharged. The area of electrodes discharged by the avalanche is proportional to the avalanche charge, and thus is much larger in streamer mode than in avalanche mode. Therefore operating the RPC in streamer mode must be avoided in order to work at high rates. It has been shown that efficient operation can be obtained also in avalanche mode, where the charge is limited to tens of pC [4]. Special gas mixtures, that reduce the creation of streamers, have also been developed.

2.1.4 Rate capability

Since the time constant for recharge is directly proportional to the bulk resistivity ρ of the electrodes (being of the order of milliseconds), the rate capability is proportional to $1/\rho$ and it is therefore desirable to have low-resistivity bakelite for the electrodes. Some RPCs with $\rho = 5 \cdot 10^8 \Omega\text{cm}$ have been successfully tested, however there is no large experience in this region of resistivities. For industrial bakelite resistivities $\rho > 5 \cdot 10^9 \Omega\text{cm}$ are more common, and values of $10^{10} - 10^{11}$ are used by ATLAS and CMS [5] [6].

2.2 Specific requirements

Beyond the rate capability ($2 \text{ kHz}/\text{cm}^2$), time resolution and cluster size are important requirements. The cluster size (i.e. the number of adjacent strips fired simultaneously by a crossing particle) must be small in order to minimize the load on the trigger system. The requirements for the RPC detectors are summarized in Table 1.

In order to cope satisfactorily with high rate, the resistivity of the bakelite should be as small as practicable. We propose to use bakelite with resistivity of $9 \cdot 10^9 \Omega \text{ cm}$ and thickness of 2 mm, which has been successfully tested by us and other groups up to $> 3 \text{ kHz}/\text{cm}^2$.

Table 1 LHCb requirements for RPC.

Spatial efficiency per station	$> 99\%$
Rate capability	2 kHz/cm^2
Time resolution	$\leq 2 \text{ ns}$
Average cluster size	$\leq 1.6 \text{ strips (?)}$

Higher rates could be reached with lower resistivity, and we are in contact with the producers to perform tests of the new materials as soon as they become available.

2.3 Types of detectors

We have considered two variants of the RPC detector, namely the single-gap RPC (SRPC) and the double-gap (DRPC). For both the basic building block is the gas gap, 2 mm thick and comprised between two phenolic sheets also 2 mm thick. These sheets are glued on a polycarbonate frame (7 mm wide) and round polycarbonate spacers (height 2.00 ± 0.01 mm) are glued in between, forming a rectangular grid of 100 mm pitch. The four gas inlets/outlets are placed close to the corners. A graphite layer is sprayed on the external surface of the bakelite planes in order to distribute the voltage. A PET insulating film ($200 \mu\text{m}$ thick) is glued on the bakelite layer.

The frame gives a loss of about 2 % for a $2 \times 1 \text{ m}^2$ RPC. The dead area associated with the spacers is 1 %.

In the SRPC there are usually two planes of readout strips (Fig. 3). These are placed close to the graphite (separated by the PET insulating layer)). The strips behave like transmission lines of $25\text{-}50 \Omega$ impedance and must be terminated to avoid reflections. The polarity of the signal picked up being opposite for the two planes, the front-end electronics must be designed accordingly.

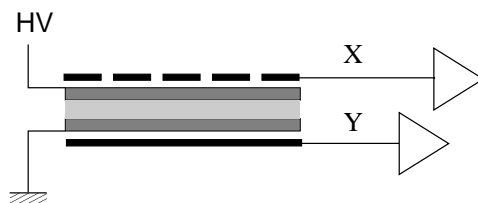


Figure 3 Layout of a single-gap RPC with two readout planes.

The idea behind the DRPC is to increase efficiency by performing an analog OR of the signals from two gas gaps. In the DRPC different strip arrangements can be used (see Fig. 4) to achieve this. In the first case the readout strip plane is sandwiched between two gas gaps [7] and therefore receives induction from both of them. In the second case the strips are on the external side and are connected together. CMS has chosen the first solution. The price to pay is two gas gaps for a single coordinate, whereas two coordinates are possible with the single plane of the SRPC. The larger efficiency of the DRPC translates into a better rate capability and into an improved timing resolution.

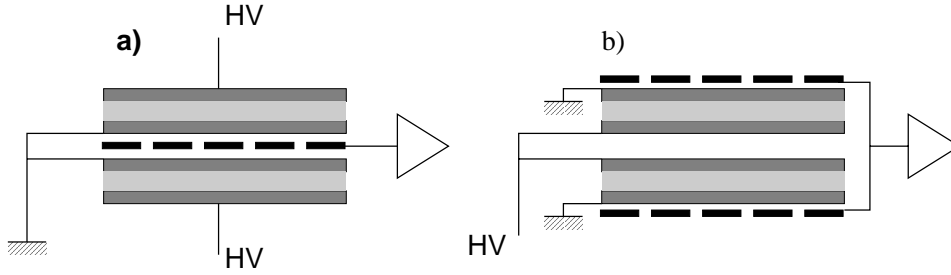


Figure 4 Layout of a double-gap RPC: a) with one readout plane, b) with two readout planes.

2.4 Detector performances

We have tested several type of detectors either on beam or at the CERN GIF facility, with particle fluxes up to 10 kHz/cm^2 [8]. The detectors (dimensions $50 \times 50 \text{ cm}$) were built with bakelite of $9 \cdot 10^9 \Omega \text{ cm}$ resistivity.

The gas mixture consisted of 95 % $\text{C}_2\text{H}_2\text{F}_4$, 4 % isobutane and 1 % SF_6 [9]. $\text{C}_2\text{H}_2\text{F}_4$ is a non-flammable, environmentally safe gas. This gas is characterized by high density and large primary ionization (> 60 primary ion pairs per cm). It has a relatively low operating voltage, low cost and easy availability. The percentage of isobutane is below the flammability threshold (5.75 %). SF_6 has the effect of reducing the formation of streamers.

For the readout electronics we used fast voltage amplifiers connected to the strips (widths of 2 and 3 cm), followed by discriminators and multi-hit TDCs. We used generally a threshold value of 60 mV, unless stated otherwise. Taking into account the preamplifier gain this corresponds to about 80 fC.

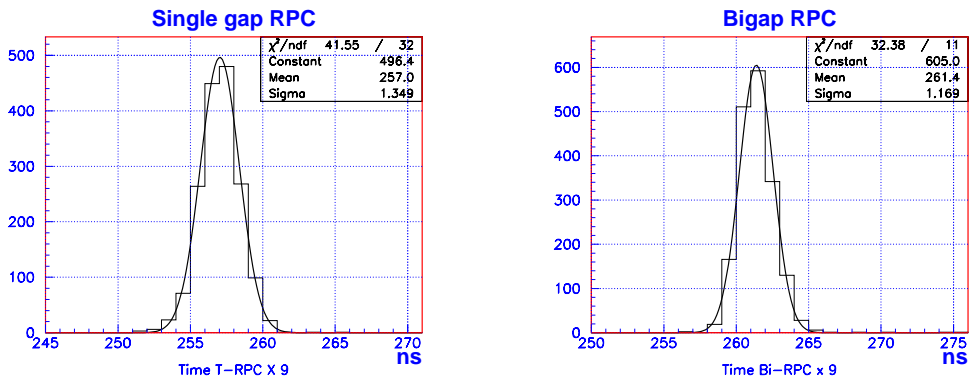


Figure 5 Time resolution for SRPC (left) and DRPC (right) (1 ns/ch)

2.4.1 Beam tests

The data have been collected at the T11 pion beam at the CERN PS. The beam was approximately round in shape, with a FWHM of about 3 cm. We took data at several different intensities of the spill, corresponding to a flux between 0.5 kHz/cm^2 and 10 kHz/cm^2 in the central region of the beam spot.

Fig. 5 shows the time resolution for the SRPC and the DRPC. The timing resolution of the trigger scintillators has not been subtracted. The values obtained are $\sigma_t = 1.35$ ns for the SRPC and $\sigma_t = 1.17$ ns for the DRPC, with negligible tails.

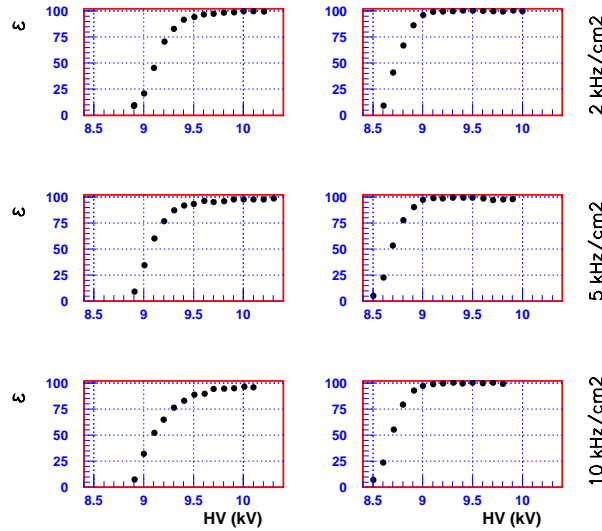


Figure 6 Efficiency curves for SRPC (left) and DRPC (right) at various beam intensities.

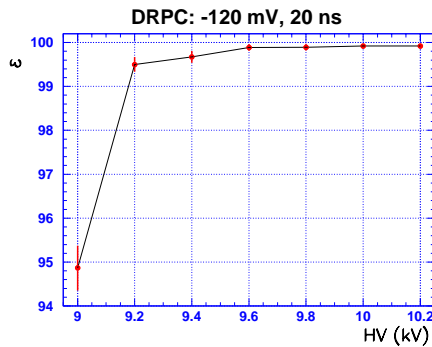


Figure 7 Efficiency curve for DRPC. Threshold 120 mV; gate: 20 ns; beam flux: 3 kHz/cm²

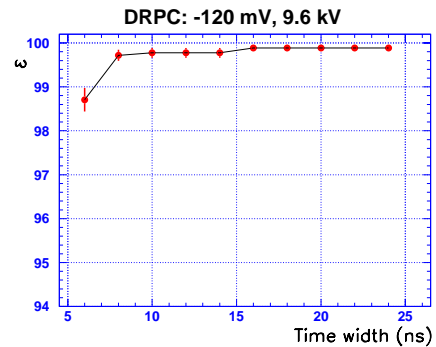


Figure 8 DRPC efficiency vs. gate width. Threshold 120 mV; HV = 9.6 kV; beam flux: 3 kHz/cm²

Fig. 6 shows the efficiency curves for the SRPC and DRPC under different beam intensity conditions. The DRPC shows clearly better efficiency at large rate, with almost no visible drop in performance up to 10 kHz/cm². The SRPC shows some efficiency drop: at 9.8 kV ϵ decreases from 98 % at 2 kHz/cm² to 96 % at 5 kHz/cm². An expanded efficiency curve for the DRPC is shown in Fig. 7.

The excellent time resolution of the detector allows to get full efficiency already for gate widths of 8 ns (see Fig.8).

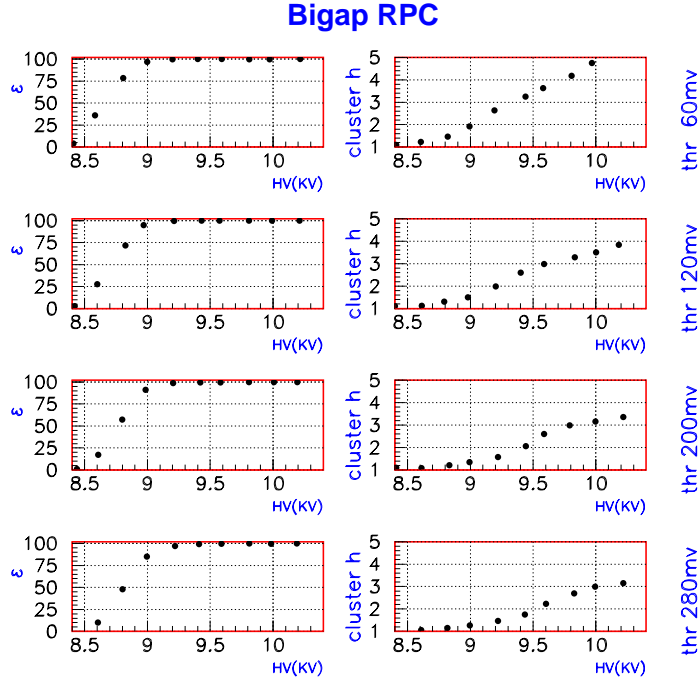


Figure 9 Efficiency curves (left) and cluster size (right) of the DRPC for different thresholds.

The average cluster size measured in our SRPC tests is $\langle h \rangle = 1.2 - 1.6$ strips. These values are slightly larger than those quoted by ATLAS. For the DRPC CMS obtains $\langle h \rangle \approx 1.5$ [6], whereas our results are considerably worse and improve only slightly by increasing the thresholds (see Fig. 9).

We believe that the discrepancy could be due to the type of electronics and will disappear when the final electronics will be used. Moreover, since the cluster width is essentially due to cross-talk between adjacent strips, some improvement could also be obtained with an optimization of the strip design (surface graphite resistivity, strip to graphite capacitance, etc.) We also point out that the cluster width does not depend on the strip size, and grouping the physical strips in larger logical strips will help. A simulation of the trigger performances with $\langle h \rangle$ in the range $1.2 - 3$ is in progress.

2.4.2 GIF tests

The GIF (Gamma Irradiation Facility) at CERN is based on a very intense (740 GBq) ^{137}Cs source. The GIF is used to test detectors under continuous photon load, with fluxes comparable to those expected by the large LHC detectors. We could only test three SRPC detectors on the facility.

The GIF setup is shown in Fig. 10. The source is placed in a protected area on the X5 SPS beam line. A system of filters can be used to adjust the intensity of the 662-keV photons and to make it reasonably uniform over the area of the detectors. In this process the energy spectrum of the photons is considerably degraded. Because of this fact, the resulting flux is not strictly linear with $1/\text{Attenuation}$ [10]. At 1 m the counting rate achieved at minimum source attenuation ($\text{Att}=1$) corresponded to a flux of charged particles (photoelectric and Compton

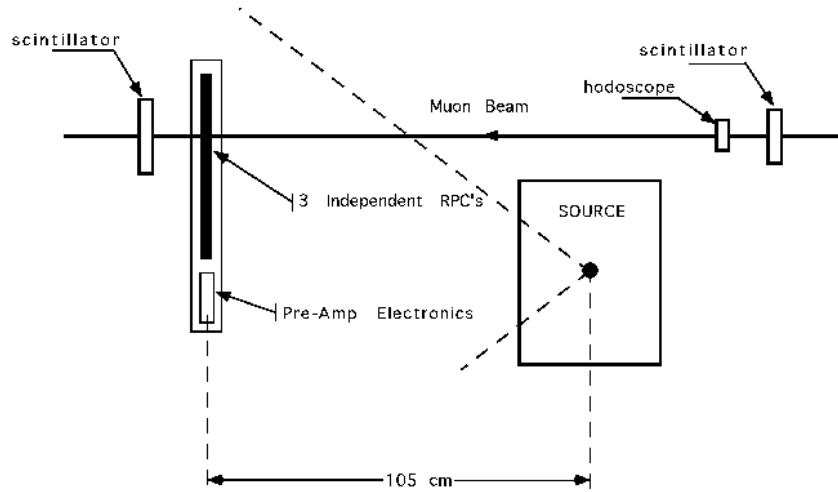


Figure 10 GIF test setup

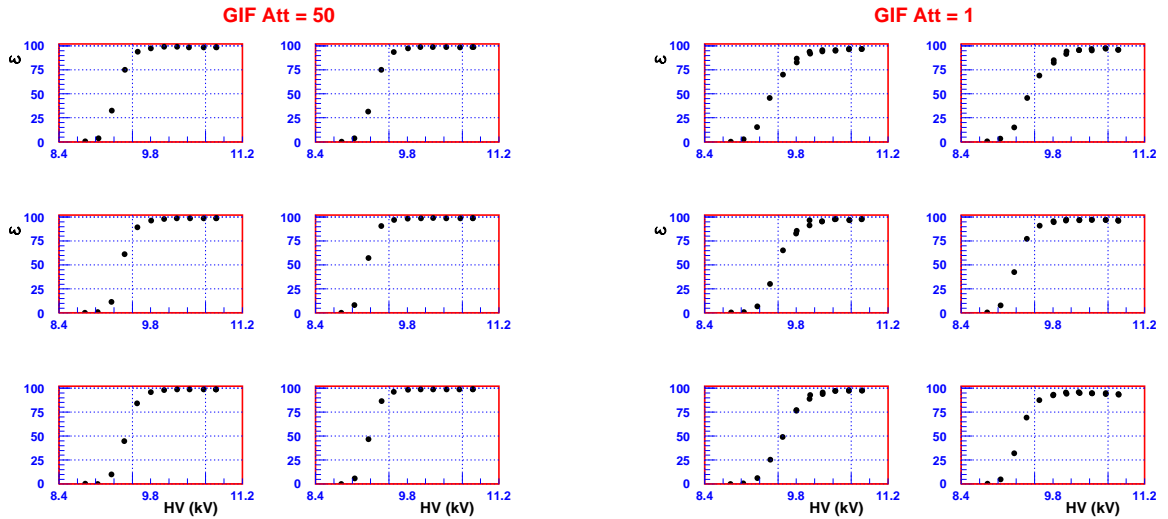


Figure 11 Efficiency curves for planes X (left) and Y (right) of the three SRPCs, for GIF attenuation 50 (flux 160 Hz/ cm²).

Figure 12 Efficiency curves for planes X (left) and Y (right) of the three SRPCs, for GIF attenuation 1 (flux 3.1 kHz/ cm²).

electrons) of 3.1 kHz/ cm². The sensitivity of the RPC to photons was derived to be $\epsilon_\gamma \cong 1.2 \cdot 10^{-3}$.

The efficiency curves for muons as a function of the HV, with GIF Att = 50 and Att = 1 are shown in Fig. 11 and 12 for the X and Y readout of the three RPCs. At Att = 1 the onset of the plateau is displaced by about 400 V with respect to source off conditions. It has to be considered that, beyond the 1 % loss due to the spacers, at Att=1 the rate on the strips was as high as 800 kHz, introducing a dead time loss of about 3 %. The correction due to random was -1.5 %. In these conditions the three chambers still reach > 95 % efficiency. At 10 kV the currents drawn by the chambers were about 0.2, 0.4 and 0.3 mA, corresponding to average cluster charges of 25-50 pC as expected for the avalanche mode of operation..

2.5 Ageing properties

The mechanism of ageing in RPCs is different from that of wire chambers, and in first approximation is related to changes in the characteristics of bakelite. In particular, increases of resistivity could affect the rate capability of the chambers.

RPCs have been in use for several years in L3 and no degradation of the performances has been detected, so dramatic changes of the electrical properties of bakelite due to “natural” ageing seem unlikely. Effects due to irradiation are probably more important in LHCb, since they could produce a variation of the resistivity. Less likely appears that the current flowing for long time inside the bakelite could affect its properties.

According to Monte Carlo simulations, and taking into account the various safety factors, the maximum integrated dose in ten years for the RPC detectors of LHCb is about 30 Gy.

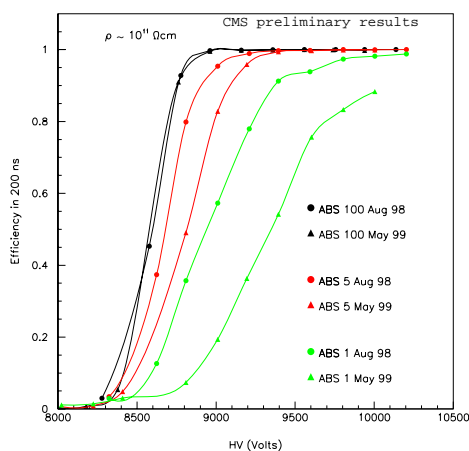


Figure 13 Efficiency curves for the CMS RPC before (circles) and after (triangles) irradiation at the GIF [11]. Total dose: 20 Gy. Flux values from 0.1 to 5 kHz/cm² (see text).

CMS has recently performed measurements on the GIF over a period of $7 \cdot 10^6$ s, using an RPC with large resistivity ($4 \cdot 10^{11} \Omega\text{cm}$, so not well suited to large rates). The efficiency curves have been measured at different incident flux before and after exposition to the gamma source (see Fig. 13). With a total absorbed dose of 20 Gy, there was a 10 % loss of efficiency at the largest flux of 5 kHz/cm² (Att=1) but a negligible effect at 1.3 kHz/cm² (Att=5). The effect is understandable as a change of the bakelite resistivity, and should be greatly reduced in the case of LHCb where the resistivity will be 40 times less.

3 RPC construction

There is today a wide experience in industrial production of RPCs. The procedure for construction and the necessary tooling was developed several years ago by R. Santonico in collaboration with industry, and was successfully used in L3 and BABAR. This procedure has been continuously refined by R&D work for ATLAS and CMS, so we are confident that the production of the RPCs gaps can be made in industry. The production process has however to be closely monitored to ensure the quality of the chambers. In particular, the selection of the bakelite (resistivity and surface roughness) will be under the direct responsibility of the institutes. For the details of manufacturing, please refer to the ATLAS and CMS TDRs [5],[6].

The production capability in the industry is about 15 single-gaps/day. This is adequate for us, since the total number of single-gaps needed is about 900 (see below).

4 Station layout

Due to the relatively high rate, we think that a double-gap solution is the most appropriate in LHCb. The performance of single-gap RPC is in fact marginal at 2 kHz/cm², making necessary to employ more than one gas layer to obtain the required efficiency (see Table 1).

The simplest way to combine two gas gaps is in fact the DRPC. Solutions like the majority of 3 SRPC planes have been considered, but they are more complicated and expensive, and the advantage in terms of random noise suppression does not seem to be enough to justify them.

Moreover DRPCs have slightly superior timing performances than SRPC (see Figs. 5 and 8) and this is very important for correct bunch-crossing identification.

DRPCs can be operated at lower voltage than SRPC (about 500 V less), therefore the HV supply does not need to exceed 10 kV and the power dissipation under intense load conditions is smaller.

Finally, the use of two separate gas gaps per readout plane, which will be powered independently, offers excellent flexibility and redundancy.

The increase in number of hits due to the presence of the OR is small since most of the background is correlated and therefore it is anyway seen in the two chambers. This solution also minimizes the number of front-end physical channels and simplifies the subsequent electronics.

4.1 Chamber dimensions

The layout in the four stations M2 – M5 is based on chambers with two separate layers of DRPC (one for the X and one for the Y coordinate), thus requiring 4 gas gaps. The total thickness available between the iron plates is 360 mm. An alternative, discussed below, uses only 3 gas gaps in each chamber and allows a more compact arrangement. Calling ε the efficiency of a single-gap, the spatial efficiency for the chamber can be expressed as: $\varepsilon_{X,Y} = \varepsilon^2(4 - 4\varepsilon + \varepsilon^2)$. This gives $\varepsilon_{X,Y} = 99\%$ for $\varepsilon = 93\%$.

From the point of view of construction, there is an advantage in using the largest detectors as possible. The use of large chambers minimizes the extension of boundaries and helps in reducing the effect of dead spaces. The commercial bakelite dimensions and the tooling available in the industry sets the upper limit at $1.25 \times 3.2 \text{ m}^2$. On the other hand, the maximum strip lengths in LHCb limits in practice the size of the chambers to $1.25 \times 1.5 \text{ m}^2$, unless larger chambers with strips split in the middle are used.

A readout with split strips will introduce some construction problems for long strips, that must be terminated at both ends, but could be possible for small chambers, and is a possible option for chambers in Region III (see below).

The propagation delay of 5.5 ns/m yields for the longest strips a time spread of 8.25 ns, small enough to avoid any problem of bunch identification.

The proposed layout of the stations assumes to have in M2 chambers of $1.2 \times 1 \text{ m}^2$, and appropriately scaled in M3 – M5. This shall also allow to keep the HV current requirement below 1 mA per chamber. Table 2 gives the detailed list of dimensions and the number of the chambers.

A second option is to have smaller chambers in Region III (half the size of one or both sides), if the strip lengths have to be reduced because of problems of occupancy in the trigger or because of dead-time, and if the strips cannot simply be split in two. In that case the number of chambers could increase.

4.2 Dead spaces

In order to minimize dead space effects at the boundary between two readout planes, a possible solution can be seen in Fig. 14. The gas gaps are staggered along a direction, the vertical for

Table 2 Chamber sizes for the RPC stations. A single “chamber” is made of 4 (or 3) gas gaps (see text).

Station	Region	No. chambers	X dim (mm)	Y dim (mm)	Area (m ²)
M2	IV	48	1200	1000	58
M3	III	12	1300	1080	17
M3	IV	48	1300	1080	68
M4	III	12	1400	1160	20
M4	IV	48	1400	1160	78
M5	III	12	1500	1240	22
M5	IV	48	1500	1240	89
Total		228			352

example, in such a way that the readout strip layer always sees at least one gas gap. In this way the transition zone will have a slightly reduced efficiency (better however in most cases than 95 %) and the total loss is a second-order effect. The orientation of the strips (x or y) has of course no relationship with the direction along which the overlap occurs.

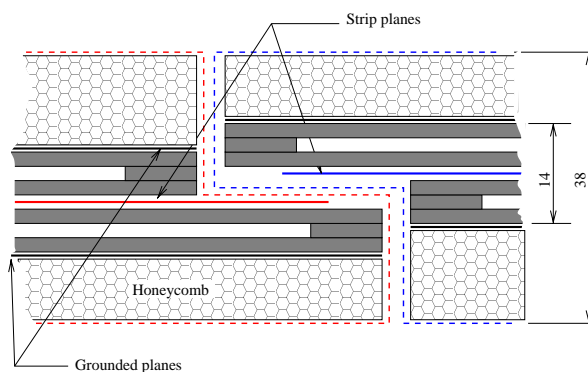


Figure 14 Overlapping region of DRPC readout planes.

The assembly is kept in place by means of honeycomb support panels that ensure the necessary rigidity to all the chamber structure. The completed chamber has a thickness of about 40 mm. Along the orthogonal (the horizontal) direction the dead space is avoided by overlapping the chambers like in Fig. 15. Since this has to be repeated separately for the chamber measuring the two coordinates a space along Z of $40 \times 4 = 160$ mm is required, easily accommodated in between the iron absorber (360 mm available).

A more attractive/elegant solution makes use of only 3 gas gaps, assembled in such a way that each strip plane sees two gaps (Fig. 16). In this way the middle gap is shared by two strip planes (x and y) and it is possible to spare one gap. We call this solution TRPC. The assembly of one TRPC chamber requires 52 mm thickness, and the overall space needed along Z is thus only $52 \times 2 = 104$ mm.

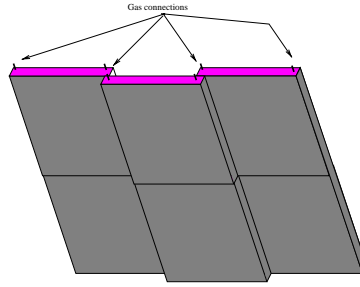


Figure 15 Overlapping of the chambers.

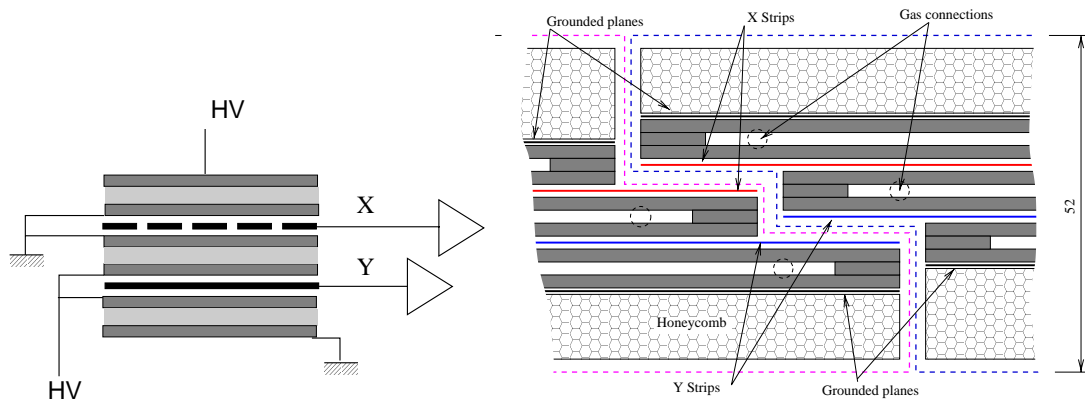


Figure 16 Principle of the triple-gap RPC with X and Y readout planes (left). Practical solution for the overlapping region (right).

4.3 Readout strips

The width of the readout strips must be an integer fraction of the logical strip width. We have chosen the fraction in such a way to have strip sizes not much different from 3 cm, thus maintaining the same impedance everywhere (about 30Ω). The size of the vertical and horizontal strips is the same in every station.

The number of physical strips participating in a logical strip varies between 1 (for the strips measuring x in region III of M2 and M3) and 10. The length of the strips will be equal to the chamber side, or it could be half of it if the strips can be used without termination on one end (this can only occur for half-meter strips). Table 3 gives the strip widths and the total number of channels. There are however two factors limiting the size of the strips, namely (i) the maximum counting rate allowed on the front-end channels and (ii) the cluster size.

(i) is strictly connected with the dead time introduced by the front-end electronics and with the fact that the present design of the trigger is extremely demanding in terms of station efficiency. It must be stressed that RPC, being fast in response ($\simeq 5$ ns pulse width), are much better in this respect than MWPC, provided the appropriate electronics is used (see below).

Concerning (ii), in case that the cluster size is excessive, the width of the x strips can be halved, with a modest increase in the number of front-end channels. It is likely that (ii) will not constitute a problem once (i) will be taken into account. So the numbers of Table 3 must be considered provisional.

Table 3 Tentative trip sizes and physical channel count for the RPC stations (see text).

Station	Region	No. chambers	X strip (cm)	Strips/RPC (X)	Y strip (cm)	Strips/RPC (Y)	Total channels
M2	IV	48	2.5	48	2.5	40	4224
M3	III	12	2.7	48	2.7	40	1056
M3	IV	48	2.7	48	2.7	40	4224
M4	III	12	2.9	48	2.9	40	1056
M4	IV	48	2.9	48	2.9	40	4224
M5	III	12	3.1	48	3.1	40	1056
M5	IV	48	3.1	48	3.1	40	4224
Total		228					20064

4.4 Chamber production

The assembly of the RPC gas gaps and of the strips to form a complete chamber will be made in the industry. These chambers will then be delivered to the institute laboratories, where the front-end electronics will be mounted. Finally several chambers in parallel will be tested with cosmic rays. From six to twelve months should be necessary to perform this task. The chambers will then be shipped to CERN.

4.5 Station assembly

This will be made at CERN.

5 RPC front-end electronics

Two possibilities exist: (1) the ATLAS chip and (2) the CMS chip. Both chips have 8 channels comprising integrated amplifier-shaper-discriminator and have been designed specially for RPCs. Circuit (1) is built in GaAs and is only available in die form, thus requiring to be bonded to the circuit board.

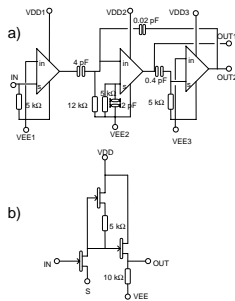


Figure 17 Block diagram of the ATLAS front-end GaAs chip: a) interconnection of the three stages; b) sketch of the single stage.

It is a voltage amplifier followed by a discriminator and output circuit (Fig. 17), and requires a step-up transformer as a part of the multilayer front-end board to adapt the strip impedance to the input. The necessity of bonding and of the step-up transformer are complications whose associated extra costs need to be carefully evaluated, even if the chip itself has a very attractive price.

Circuit (2), built in BiCMOS technology, is shown schematically in Fig. 18. The transimpedance preamplifier is adapted to the strip line and is followed by a zero-crossing discriminator and LVDS driver. It comes in a PQFP 80 64-pin plastic case [12].

Concerning the rate capability, circuit (1) should be capable of operating up to 100 MHz, whereas circuit (2) has a monostable in the output circuit which introduces a dead time of 70 ns.

We plan to test both circuits and to carefully compare their performances in connection with our DRPC detectors. In particular (i) the time resolution, (ii) the dead-time requirements and (iii) the cluster width will be considered in the comparison.

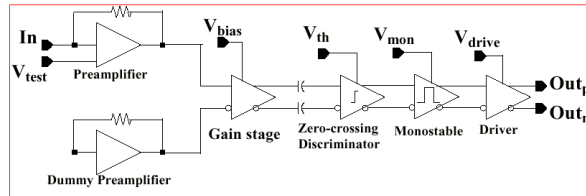


Figure 18 Block diagram of the CMS front-end BiCMOS chip.

6 HV system

7 Gas system

References

- [1] LHCb Technical Proposal, CERN/LHCC 98-4, 1998.
- [2] R. Santonico and R. Cardarelli, Nucl. Instr. and Meth. in Phys. Res. 187 (1981) 377.
- [3] R. LeGac, A. Tsaregorodtsev, V. Talanov, LHCb Note 99-036 (1999).
- [4] R. Cardarelli, A. Di Ciaccio and R. Santonico, Nucl. Instr. and Meth. in Phys. Res. A 333 (1993) 399;
C. Bacci et al., Nucl. Instr. and Meth. in Phys. Res. A352 (1995) 552;
R. Cardarelli, V. Makeev, R. Santonico, Nucl. Instr. and Meth. in Phys. Res. A 382 (1996) 470.
- [5] ATLAS muon TDR, CERN/LHCC/97-22, 1997.
- [6] CMS muon TDR, CERN/LHCC/97-32, 1997.
- [7] T. Moers et al., Nucl. Instr. and Meth. in Phys. Res. A 345 (1994) 474.
- [8] M. Adinolfi et al., LHCb Note 99-049, 1999.
- [9] P. Camarri et al. Nucl. Instr. and Meth. in Phys. Res. A 414 (1998) 317.
- [10] When scaled for the different distances, our results agree with those reported by M. Maggi et al, Proc. IV Int. Workshop on RPC and Related Detectors, Scientifica Acta Univ. Pavia, vol XIII n.2 (1998) 139.
- [11] G. Pugliese, talk given at the 5th Int. Conf on Position-Sensitive Detectors, London (1999).
- [12] F. Loddo, talk given at the V Int. Workshop on RPC and Related Detectors, Bari (1999).